Microstructure and texture of a severely warm-rolled and annealed AlCoCrFeNi2.1 eutectic high entropy alloy

(article starts on next page)

PAPER • OPEN ACCESS

Microstructure and texture of a severely warm-rolled and annealed AlCoCrFeNi$_{2.1}$ eutectic high entropy alloy

IOP ebooks™

Bringing you innovative digital publishing with leading voices to create your essential collection of books in STEM research.

Start exploring the collection - download the first chapter of every title for free.

Microstructure and texture of a severely warm-rolled and annealed AlCoCrFeNi$_{2.1}$ eutectic high entropy alloy

S R Reddy [1, a], U Sunkari [1], A Lozinko [2], S Guo [2], P P Bhattacharjee [1, b]

[1] Department of Materials Science and Metallurgical Engineering, IIT Hyderabad, Kandi, Sangareddy, 502285, Telangana, India

[2] Industrial and Materials Science, Chalmers University of Technology, 41296 Gothenburg, Sweden

E-mail: ([a] ms14m16p000001@iith.ac.in, [b] pinakib@iith.ac.in)

Abstract. The effect of warm-rolling and subsequent annealing on the evolution of microstructure and texture was systematically investigated in a lamellar (L1$_2$+B2) AlCoCrFeNi$_{2.1}$ eutectic high entropy alloy (EHEA). The EHEA was warm-rolled at 400°C up to 90% reduction in thickness and annealed at different temperatures. Ultra-fine lamellar microstructure evolved after heavy deformation with the characteristic textures of the two phases. Annealing treatments resulted in the gradual development of an ultrafine micro-duplex structure with increasing annealing temperature, even though the alloy showed significant resistance to grain growth. The annealing process was featured by concomitant microstructural and textural changes.

1. Introduction

High entropy alloys (HEAs) are a new class of multicomponent alloys containing a large number of alloying elements ($\geq$5) in equiatomic or near equiatomic proportions [1]. HEAs may show simple phases owing to their large configurational entropy [1, 2]. HEAs have shown tremendous potential due to their intriguing and attractive mechanical properties.

Eutectic HEAs (EHEAs) are a special class of HEAs developed due to their excellent castability and enhanced properties [3]. AlCoCrFeNi$_{2.1}$ EHEA is found to show superior mechanical properties due to the presence of ordered L1$_2$ (soft) and B2 (hard) phases [3, 4]. Thermo-mechanical processing comprising of heavy deformation (cold/cryo) and annealing [4-7] led to the development of tailored microstructures exhibiting superior strength-ductility synergy in these alloys. However, the effect of warm-rolling on the microstructure of these EHEAs has not been studied intensively, which constitutes the major objective of the present research.

2. Experimental procedure

The AlCoCrFeNi$_{2.1}$ EHEA used in the present work was prepared by arc melting from high purity elements followed by suction casting. Specimens with dimensions 20mm*15mm*3mm were extracted from the as-cast EHEA followed by isothermal warm-rolling at 400°C up to 90% reduction in thickness (~0.3mm) using a laboratory scale two-high rolling machine (SPX Precision Instruments, Fenn, USA). The 90% warm-rolled samples were annealed at different temperatures ranging between 800°C to 1200°C for 1 h.

The microstructure and texture of the deformed and annealed samples were investigated using an electron backscatter diffraction (EBSD) system (Oxford Instruments, UK) attached to a Field Emission Gun-Scanning Electron Microscope (FEG-SEM) (SUPRA 40, Carl-Zeiss, Germany). The samples for SEM-EBSD were prepared by mechanical polishing up to colloidal silica followed by electro-polishing using an electrolyte mixture of 90% ethanol + 10% perchloric acid. Several EBSD scans were acquired and analyzed by the TSL-OIM^{TM} (EDAX, USA) software. The orientation distribution functions (ODFs) were calculated using a harmonic series expansion method (series rank 22) using orthotropic sample symmetry. The hardness measurements of the deformed and annealed samples were performed using micro Vickers Hardness Tester (DuraScan 20, Emco-Test, Austria).

3. Results and discussion

Figure 1 shows the EBSD image quality (IQ) maps of the as-cast EHEA and those following warm-rolling to different thickness reductions. The as-cast EHEA reveals the eutectic mixture (65:35) of L1$_2$ /ordered FCC (white) and B2/ordered BCC (dark) phases as shown in figure 1 (a). The average lamellar spacing of the as-cast EHEA is 0.36 μm with a hardness of 330 Hv. The EHEA shows progressive alignment of the lamellae along the rollig direction with increasing thickness reduction as shown by the IQ maps of the 20% (figure 1(b)) and 50% (figure 1(c)) reduction in thickness. The development of ultra-fine lamellar microstructure can be observed after 90% deformation (figure 1(d)). Presence of shear bands are also easily seen in the microstructure.
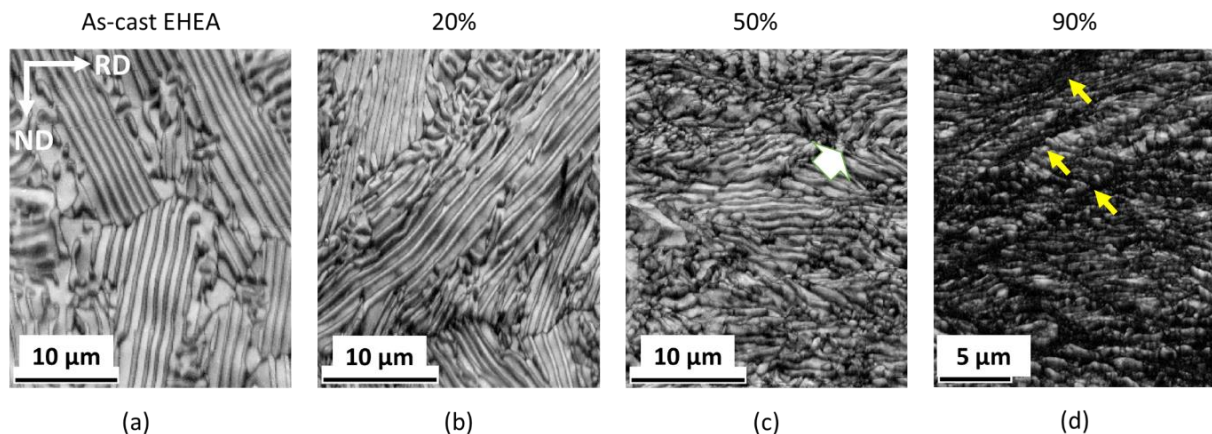

Figure 1. EBSD image quality (IQ) maps showing microstructure of (a) as-cast, (b) 20%, (c) 50% and (d) 90% warm rolled EHEA. The IQ maps confirms the L1$_2$ /FCC (white) and B2 (dark) phase.
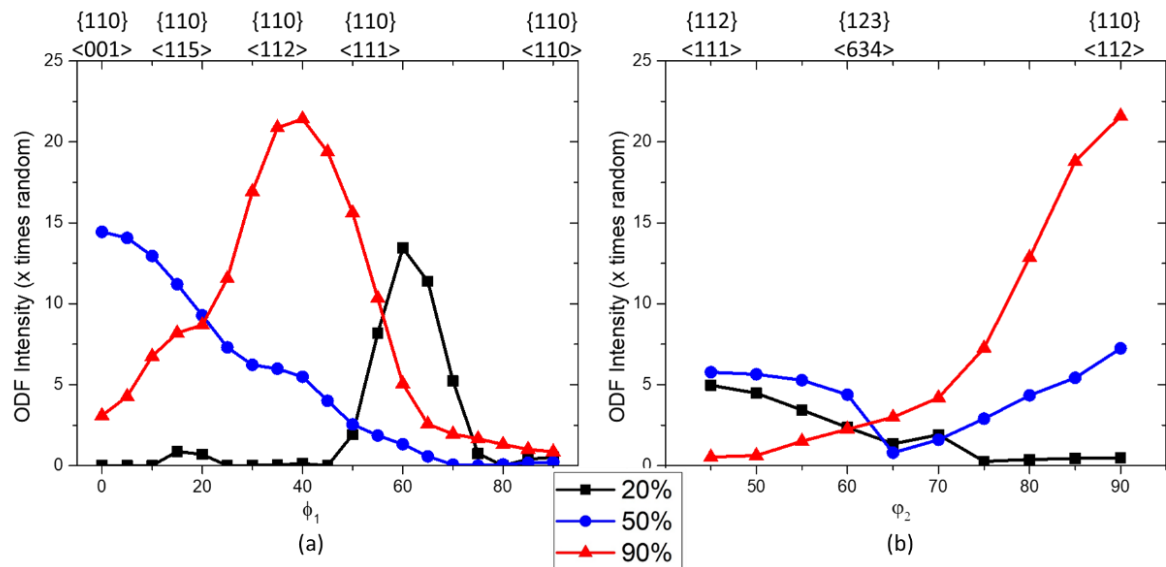
Figure 2. Change in intensities along the (a) α-fiber and (b) β-fiber of the L1$_2$/FCC phase in the EHEA with increasing deformation. The locations of important texture components in L1$_2$/FCC phase are indicated.
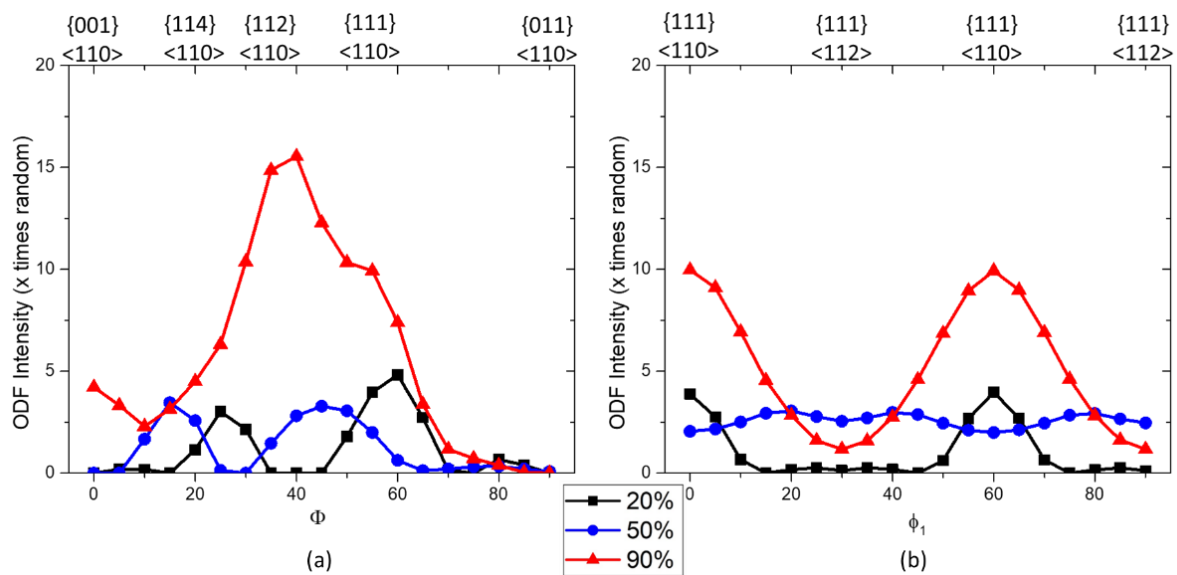

Figure 3. Change in intensities along the (a) RD-fiber (//<110>) and (b) ND-fiber (//<111>) of the B2/BCC phase in the EHEA with increasing deformation. The locations of important texture components in B2/BCC phase are indicated.

In order to understand the texture development during deformation, relevant texture fiber plots of the L1$_2$/FCC phase are represented in figure 2. The α-fiber plot (extending from Goss {011}<001> to Brass orientation {110}<112>) (figure 2(a)) confirms the development of strong Brass ({110}<112>) after 90% deformation. The β-fiber plot (extending from Copper {112}<111> to S {123}<634> to Brass orientation) (figure 2(b)) [8] also confirms the strong intensity of the Brass component. Evidently, the L1$_2$/FCC phase develops predominantly Brass type deformation texture.

Figure 3 shows relevant texture fiber charts (a) RD-fiber (//<110>) (extending from {001}<110> to {111}<110>) and (b) ND-fiber (//<111>) (extending from {111}<110> to {111}<112>) of the B2 phase of the warm rolled materials. The increase in deformation up to 90% led to the development of typical RD and ND-fiber with strong intensities of the RD-fiber centered on {112}<110> while the ND-fiber centered on {111}<110>. Therefore, the B2 phase shows typical RD and ND-fiber components.
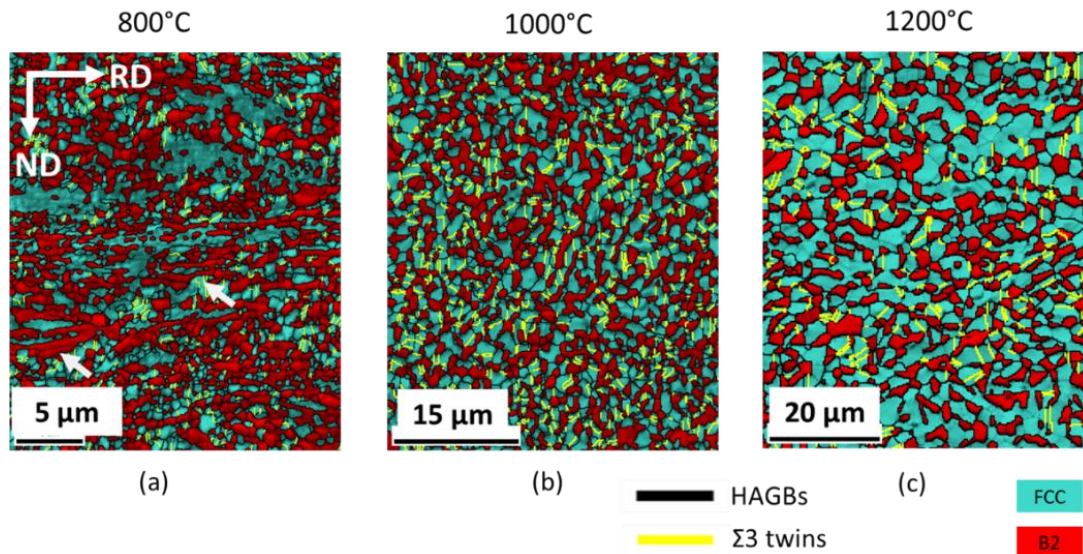

Figure 4. EBSD phase maps of the 90% warm-rolled EHEA annealed at (a) 800°C, (b) 1000°C and (c) 1200°C for 1 hr.

Table 1: Summary of key microstructural parameters of EHEA in deformed and annealed conditions

Material Condition	Phase Fraction (FCC:BCC)	Grain size (µm)	CSL Fraction	Hardness (Hv)
90% warm-rolled	65:35	0.12 ± 0.01	-	648 ± 19
Annealed at 800°C	48:52	0.42 ± 0.02	0.16	446 ± 16
Annealed at 1000°C	55:45	0.84 ± 0.01	0.27	362 ± 11
Annealed at 1200°C	63:37	1.59 ± 0.10	0.28	325 ± 11

Figure 4 shows the EBSD phase maps of 90% warm-rolled material after annealing at 800°C (figure 4(a)), 1000°C (figure 4(b)) and 1200°C (figure 4(c)) respectively. The phase maps show the development of micro-duplex structure consisting of $L1_2$/FCC and B2 phases in 800°C with remnant extended bands as indicated by the white arrow. The material shows an ultrafine grain size of 0.4 µm after annealing at 800°C. Annealing at 1000°C and 1200°C results in the development of the duplex

structure with a systematic decrease in the B2 phase fraction. The increase in the coincidence site lattice (CSL) fraction with increasing annealing temperature is clearly observed. The EHEA shows significant resistance to the grain growth with an average grain size of ~1.6 µm at 1200°C. Systematic decrease in hardness with increasing annealing temperature is established. Table 1 summarizes the key microstructural parameters after annealing.
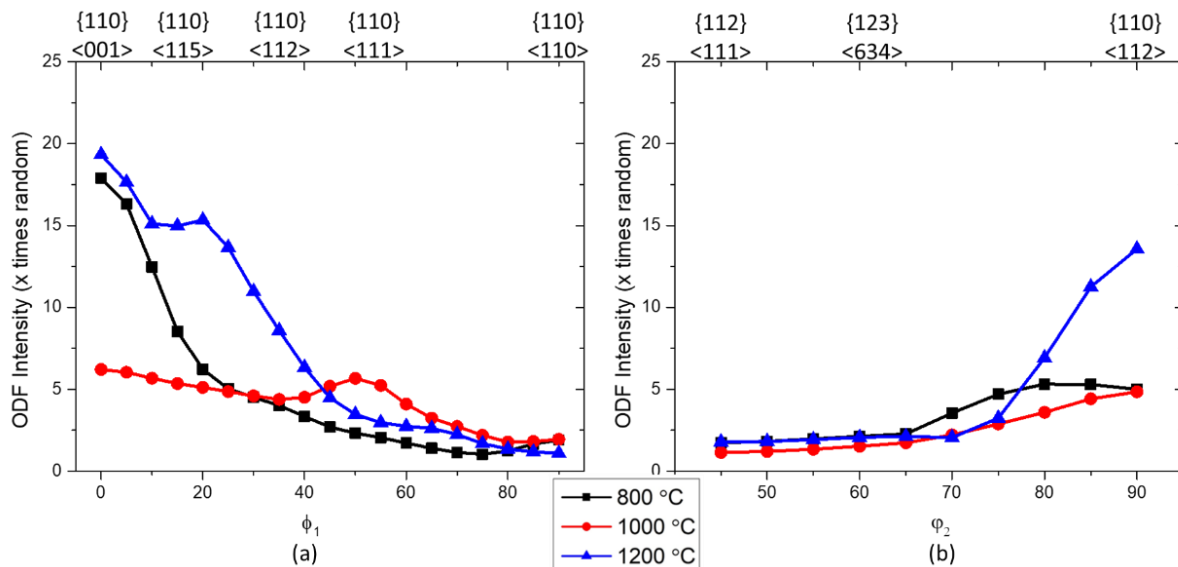

Figure 5. Intensities along the (a) α-fiber and (b) β-fiber of the L1$_2$/FCC phase in the 90% warm rolled EHEA annealed at different temperatures. The locations of important texture components in L1$_2$/FCC phase are indicated.
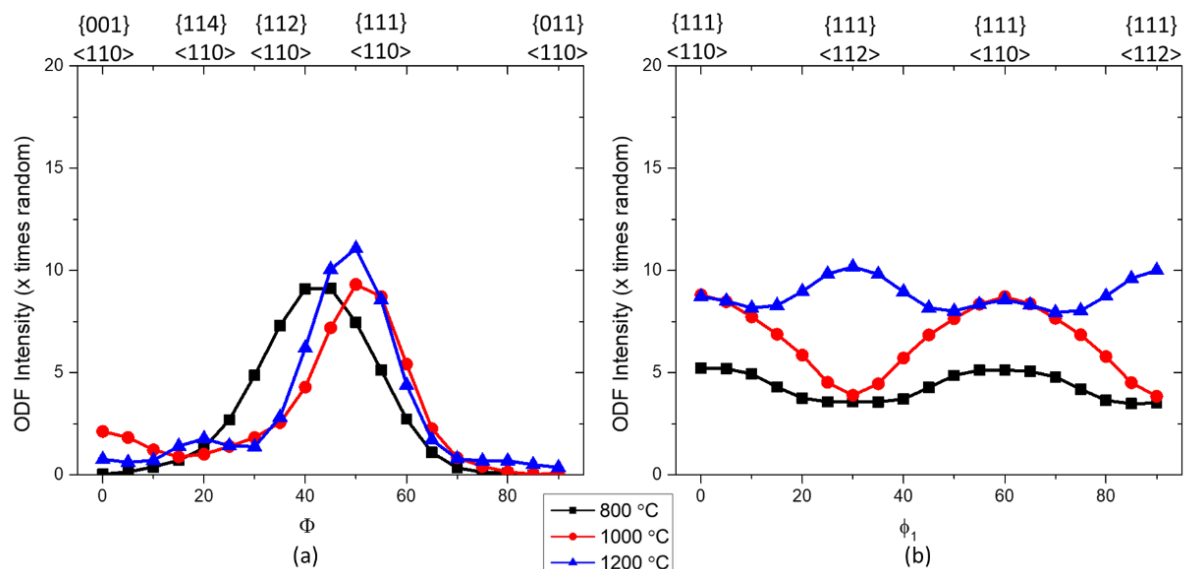

Figure 6. Intensities along the (a) RD-fiber (//<110>) and (b) ND-fiber (//<111>) of the B2/BCC phase in 90% warm rolled EHEA annealed at different temperatures. The locations of important texture components in B2/BCC phase are indicated.

The annealing texture of L1$_2$ phase is shown in figure 5. The α-fiber plot (figure 5(a)) shows strong intensities in between the Goss ({110}<001>) and Brass component. The retention of the Brass component can be confirmed from the β-fiber plot (figure 5(b)). Therefore, the deformation texture is mostly retained.

The texture evolution of the B2 phase as represented by the RD-fiber (figure 6 (a)) and ND-fiber (figure 6(b)) plots. The RD-fiber plot shows the presence of the strongest texture development at {112}<110> after 800°C, which confirms the retention of deformation texture. However, there is a shift to {111}<110> texture component with increasing annealing temperature. Stronger ND-fiber texture is confirmed upon further annealing up to 1200°C.

4. Conclusions

- Severe warm-rolling up to 90% reduction in thickness results in a gradual alignment of the lamellae along the RD.
- The L1$_2$ phase developed α-fiber (ND//<110>) texture, while the B2 phase developed the typical RD (//<110>) and ND (//<111>) fiber texture.
- Annealing resulted in the development of ultrafine duplex structure .
- The L1$_2$ phase retained the α-fiber texture, while the B2 phase displayed stronger ND-fiber texture throughout the annealing temperatures.

References

[1] Yeh J W, Chen S K, Lin S J, Gan J Y, Chin T S, Shun T T, Tsau C H, Chang S Y, 2004 *Adv. Eng. Mater.* **6(5)** 299-303.

[2] Murty B S, Yeh J W, Ranganathan S, Bhattacharjee P P, 2019 *High-entropy alloys* (London: Butterworth-Heinemann, Elsevier).

[3] Lu Y, Dong Y, Guo S, Jiang L, Kang H, Wang T, Wen B, Wang Z, Jie J, Cao Z, 2014 *Sci. Rep.* **4** 6200.

[4] Wani I S, Bhattacharjee T, Sheikh S, Lu Y P, Chatterjee S, Bhattacharjee P P, Guo S, Tsuji N, 2016 *Mater. Res. Lett.* **4(3)** 174-179.

[5] Bhattacharjee T, Wani I S, Sheikh S, Clark I T, Okawa T, Guo S, Bhattacharjee P P, Tsuji N, 2018 *Sci. Rep.* **8(1)** 3276.

[6] Patel A, Wani I S, Reddy S R, Narayanaswamy S, Lozinko A, Saha R, Guo S, Bhattacharjee P P, 2018 *Intermetallics* **97** 12-21.

[7] Wani I S, Bhattacharjee T, Sheikh S, Bhattacharjee P P, Guo S, Tsuji N, 2016 *Mater. Sci. Eng. A* **675** 99-109.

[8] Sidor J J, Kestens L A I, 2013 *Scr. Mater.* **68(5)** 273-276.